

pubs.acs.org/synthbio Research Article

Engineered Production of Strictosidine and Analogues in Yeast

Joshua Misa, John M. Billingsley, Kanji Niwa, Rachel K. Yu, and Yi Tang*



Cite This: ACS Synth. Biol. 2022, 11, 1639–1649



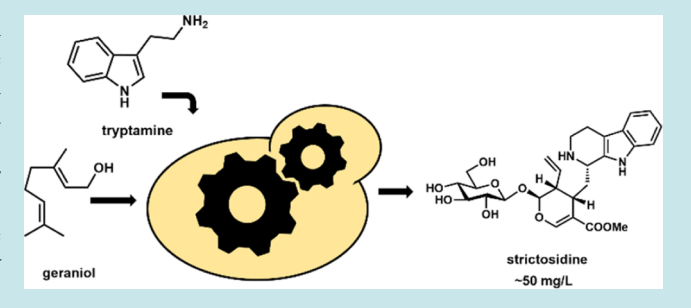
ACCESS I

Metrics & More



Supporting Information

ABSTRACT: Monoterpene indole alkaloids (MIAs) are an expansive class of plant natural products, many of which have been named on the World Health Organization's List of Essential Medicines. Low production from native plant hosts necessitates a more reliable source of these drugs to meet global demand. Here, we report the development of a yeast-based platform for high-titer production of the universal MIA precursor, strictosidine. Our fedbatch platform produces ~50 mg/L strictosidine, starting from the commodity chemicals geraniol and tryptamine. The microbially produced strictosidine was purified to homogeneity and characterized by NMR. Additionally, our approach enables the



production of halogenated strictosidine analogues through the feeding of modified tryptamines. The MIA platform strain enables rapid access to strictosidine for reconstitution and production of downstream MIA natural products.

KEYWORDS: monoterpene indole alkaloids, strictosidine, yeast, metabolic engineering, synthetic biology

■ INTRODUCTION

The use of microbial factories to produce high-value pharmaceuticals derived from plant natural products is enabled by recent advancements in synthetic biology and metabolic engineering. 1-3 Baker's yeast, Saccharomyces cerevisiae, has proven to be a particularly powerful industrial host due to its generally regarded as safe (GRAS) status, genetic tractability, and scalability. Yeast is also an attractive host because it shares a similar endomembrane system with plants, which allows for heterologous expression of plant cytochrome P450 enzymes that are often responsible for generating the chemical complexity that confers potent biological activity.^{5,6} Recently, a number of complex plant natural products have been produced from engineered yeast, including tropane alkaloids such as scopolamine, benzylisoquinolines such as hydrocodone⁸ and noscapine,⁹ sesquiterpene lactones such as artemisinin, 10 and monoterpene indole alkaloids (MIAs). 1

Strictosidine (Figure 1) is the universal precursor to thousands of structurally diverse MIAs found across many plant families. ¹² A notable MIA producer is the flowering subshrub, *Catharanthus roseus*, from the Apocynaceae family, which is known to biosynthesize the potent anti-cancer natural products vincristine and vinblastine. ¹² However, these bioactive MIAs, as well as strictosidine itself, accumulate at trace amounts in their native producers and are difficult to isolate. Given its central role in the biosynthesis of MIAs, access to a scalable route for producing strictosidine is highly desirable for both research and industrial applications. While a number of strategies have been developed to chemically synthesize strictosidine and analogues, ^{13–15} these multistep routes are difficult to scale and have low overall yields. Yeast

expressing strictosidine synthase (STR, vide infra) was used in the biotransformations of secologanin from plant extracts into strictosidine. However, secologanin is prohibitively expensive as a pure starting material, while the plant extracts are not readily available or scalable. Hence, microbial biosynthesis of strictosidine from easily accessible starting materials is an attractive approach.

The 11-step strictosidine biosynthetic pathway has been fully elucidated and characterized over the past few decades. The first committed step in strictosidine biosynthesis in planta is the formation of the monoterpene geraniol through hydrolysis of geranyl pyrophosphate (GPP) by geraniol synthase (GES) (Figure 1).18 Geraniol undergoes hydroxylation by the P450 geraniol 8-hydroxylase (G8H), oxidation of both alcohols to the dialdehyde 8-oxogeranial by 8hydroxygeraniol oxidoreductase (GOR), and reductive cyclization to the key intermediate nepetalactol by iridoid cyclase (ISY). 19-23 The recently discovered major latex protein-like (MLPL) enzyme accelerates the cyclization to nepetalactol and prevents shunt product formation.²³ Nepetalactol is then oxidized by the P450 iridoid oxidase (IO) to 7-deoxyloganetic acid, followed by a protective glucosylation step catalyzed by 7deoxyloganetic acid glucosyltransferase (7DLGT) to give 7deoxyloganic acid.²¹ Hydroxylation by the P450 7-deoxylo-

Received: January 21, 2022 Published: March 16, 2022



Figure 1. Biosynthetic pathway of strictosidine. GES: geraniol synthase; G8H: geraniol 8-hydroxylase; GOR: 8-hydroxygeraniol oxidoreductase; ISY: iridoid cyclase; MLPL: major latex protein-like; IO: iridoid oxidase; 7DLGT: 7-deoxyloganetic acid transferase; 7DLH: 7-deoxyloganic acid hydroxylase; LAMT: loganic acid *O*-methyltransferase; SLS: secologanin synthase; STR: strictosidine synthase; CPR: cytochrome P450 reductase; CYBS: cytochrome *b*5; CYPADH: cytochrome P450 alcohol dehydrogenase; UDP-Glc: uridine diphosphate glucose; SAM: *S*-adenosylmethionine.

ganic acid hydroxylase (7DLH) and methylation by loganic acid *O*-methyltransferase (LAMT) afford loganin. ^{21,24,25} An additional P450, secologanin synthase (SLS), catalyzes the oxidative ring opening to reveal the aldehyde in secologanin, which can be coupled to tryptamine *via* a Pictet–Spengler reaction catalyzed by STR to finally give strictosidine. ^{25–27}

The strictosidine biosynthetic pathway was reconstituted in yeast by O'Connor's lab. 11 Notwithstanding this landmark achievement in synthetic biology, the engineered yeast strain produced low titers of strictosidine (~0.5 mg/L). The strain contained over 20 genetic modifications, with most heterologous genes expressed under strong, constitutive promoters. This level of constitutive expression, along with significant modifications to primary metabolism, likely imparts a significant metabolic burden on the yeast cells and contributes to suboptimal yeast growth. 28 Furthermore, the recently discovered MLPL enzyme that catalyzes stereoselective cyclization of nepetalactol was not included in the reconstituted pathway. 23

In this work, we aimed to improve the production of strictosidine from yeast using a combination of the following approaches: (1) entering the pathway via supplementation of the commodity chemical geraniol instead of de novo biosynthesis from acetyl-CoA, thereby decreasing the cellular burden and initiating the biosynthetic pathway at a high substrate concentration; (2) optimizing the promoter system to decouple yeast growth and metabolite production; (3) tuning the expression of P450 and P450 accessory enzymes required in the pathway to overcome bottleneck transformations; and (4) adding the MLPL enzyme in the pathway to minimize shunt product formation. These approaches led to ~50 mg/L strictosidine titers from the yeast with minimal impact on growth. The engineered yeast strain provides a robust route to access pure strictosidine and analogues for reconstitution of more complex downstream MIA natural products.

■ RESULTS AND DISCUSSION

Overall Strategy, Promoter, and Strain Selection. Our overall strategy is to build a yeast strain for high-titer production of strictosidine from commonly obtainable, cheap precursors while maintaining robust growth characteristics.

With regard to feedstock, despite recent advances in producing the monoterpene geraniol *de novo*, it remains challenging to accumulate the compound at high levels in yeast from GPP due to competing farnesyl pyrophosphate (FPP) formation. ^{29,30} Utilization of mixed-carbon feedstock to provide "shortcut access" to terpenoid biosynthetic pathways with increased titers has been recently highlighted in several platforms. ³¹ Also, previous reports indicate that tryptamine derived from the decarboxylation of tryptophan is a low-accumulating and transient metabolite in yeast. ^{11,32} Therefore, we identified geraniol and tryptamine as ideal feedstock to the strictosidine pathway, as both can be obtained as commodity chemicals at costs that are negligible compared with that of strictosidine and downstream MIAs.

In order to further reduce the metabolic burden of heterologous protein expression and improve yeast robustness, our strategy centered on refactoring strictosidine biosynthetic enzymes and accessory enzymes under an optimal combination of constitutive and regulatable promoters. We and others have used the inducible alcohol dehydrogenase-2 promoter (ADH2), which is heavily repressed when glucose is present, but undergoes several hundred-fold change in induction when glucose is depleted,³³ in production of secondary metabolites in yeast.³⁴ The auto-inducible ADH2 allows respiratory growth and nonrespiratory production stages to be decoupled, enabling the yeast to grow to a high density before inducing expression of biosynthetic pathway enzymes. Based on their similar strengths and induction timing, we selected a set of five interchangeable, auto-inducible promoters, ADH2p, PCK1p, ICL1p, MLS2p, and an ADH2p homologue from Saccharomyces bayanus.³⁴ Using these sequence-divergent promoters with similar induction profiles allows for the construction of multigene cassettes using yeast homologous recombination. Lastly, the yeast host yJB051 was selected as the starting point for metabolic engineering (Table 1).35 This host was modified from JHY651, which has improved respiratory growth and mitochondrial stability. 34,36 The strain yJB051 contains additional mutations that minimized the shunt product formation from geraniol to nepetalactol.

Optimizing the Expression of Pathway Accessory **Enzymes.** We first modified yJB051 to support the expression of four cytochrome P450 enzymes required in the strictosidine pathway (Figure 1). Functional expression of plant P450s in yeast is a challenging task and is often the limiting step for efficient pathway reconstitution. P450 enzymes require electron shuttling from redox partner enzymes to reduce the heme-bound iron after substrate oxidation for catalytic turnover.37,38 Three C. roseus P450 accessory enzymes were chosen to be integrated into the yeast genome. These are the cytochrome P450 reductase (CPR), cytochrome b5 (CYB5), and a putative alcohol dehydrogenase, CYPADH. While the CPR and CYB5 are responsible for electron transfer, the CYPADH was proposed to specifically improve the function of IO, which oxidizes nepetalactol to 7-deoxyloganetic acid (Figure 1).11 While these enzymes were used by Brown et al., in the first demonstration of strictosidine biosynthesis in yeast, the impacts of the expression profile on P450 function, metabolic flux, and strain health were not investigated. To clarify this, we established a reporter system in which the oxidation of fed nepetalactol by expressed IO serves as a proxy for the accessory enzyme function. Expression of IO alone in yeast did not accumulate any detectable 7-deoxyloganetic acid, likely due to the rapid unraveling of the hemiacetal connected

Table 1. Yeast Strains and Plasmids Used in This Study

1 abic 1.	reast Strains and Plasmids Used in Tims	otady
strain	genotype	reference
JHY651	BY4742; MAT α prb1 Δ pep4 Δ his3 Δ leu2 Δ ura3 Δ lys2 Δ	ref 34
yJB051	JHY651; oye2 Δ oye3 Δ ari1 Δ adh7 Δ adh6 Δ	ref 35
yJM009	yJB051; oye3 Δ :: P_{ADH2} -CPR- T_{PRM9} , P_{PCK1} -CYB5- T_{SPGS} , P_{ICL1} -CYPADH- T_{CYC1}	this work
yJM010	yJB051; oye3 Δ :: P_{TEF1} -CPR- T_{PRM9} , P_{PGK1} -CYB5- T_{SPG5} , P_{TDH3} -CYPADH- T_{CYC1}	this work
yJM025	yJM010; yprcty1-2 Δ ::P _{ICLI} -7DLGT-T _{IDPI} , P _{PCKI} -LAMT-T _{CPSI} , P _{bay_ADH2} -STR-T _{ADH1}	this work
yJM038	yJM025; his3 Δ :: P_{ADH2} -IO- T_{SPG5} , P_{ICL1} -7DLH- T_{PRM9} , P_{PCK1} -SLS- T_{CPS1}	this work
plasmid	description	reference
pJB040	2μ yeast ori; HIS3; ColE1 ori; AmpR; $P_{ADH2}\text{-}7DLH-T_{PRM9},$ $P_{PCK1}\text{-}LAMT\text{-}T_{CPS1},$ $P_{MLS1}\text{-}SLS\text{-}T_{SPG5};$ $P_{ICL1}\text{-}STR\text{-}T_{IDP1}$	this work
pJB041	2μ yeast ori; URA3; ColE1 ori; AmpR; P _{ADH2} -CPR- T _{PRM9} , P _{PCK1} -CYB5-T _{SPG5} , P _{ICL1} -CYPADH-T _{CYC1}	this work
pJB152	2μ yeast ori; URA3; ColE1 ori; AmpR; $P_{ADH2}\text{-IO-T}_{PRM9},$ $P_{ICL1}\text{-}7DLGT\text{-}T_{IDP1}$	this work
pJB154	2μ yeast ori; URA3; ColE1 ori; AmpR; P $_{\rm ADH2}\text{-}{\rm CPR-}$ $\rm T_{\rm PRM9}$	this work
pJB155	2μ yeast ori; URA3; ColE1 ori; AmpR; P_{ADH2} -CYB5- T_{PRM9}	this work
pJB156	2μ yeast ori; URA3; ColE1 ori; AmpR; P $_{\rm ADH2}\text{-}{\rm CPR-}$ $T_{\rm PRM9},$ P $_{\rm PCK1}\text{-}{\rm CYB5-}T_{\rm SPG5}$	this work
pJB157	2μ yeast ori; URA3; ColE1 ori; AmpR; P_{ADH2}-IO-T_{SPG5}, P_{ICL1}-7DLGT-T_{IDP1}, P_{MLS1}-7DLH-T_{PRM9}	this work
pJB158	2μ yeast ori; URA3; ColE1 ori; AmpR; $P_{ADH2}\text{-}IO\text{-}T_{SPG5}, \\ P_{ICL1}\text{-}7DLGT\text{-}T_{IDPI}, \ P_{MLS1}\text{-}7DLH\text{-}T_{PRM9}; \ P_{PCK1}\text{-}LAMT\text{-}T_{CPS1}$	this work
pJB204	2μ yeast ori; URA3; ColE1 ori; AmpR; $P_{ADH2}\text{-}GOR-T_{PRM9}, P_{PCK1}\text{-}ISY-T_{CPS1}, P_{MLS1}\text{-}MLPL-T_{SPGS}; P_{ADH2}\text{-}G8H-T_{IDP1}$	this work
pJM022	2μ yeast ori; URA3; ColE1 ori; AmpR; P_ADH2-IO-T_SPG5, P_ICL1-7DLGT-T_IDP1, P_MLS1-CaS65-T_PRM9	this work
pJM023	2μ yeast ori; URA3; ColE1 ori; AmpR; P_ADH2-IO-T_SPG5, P_ICL1-7DLGT-T_IDP1, P_MLS1-Ca610-T_PRM9	this work
pJM030	2μ yeast ori; URA3; ColE1 ori; AmpR; P_ADH2-IO-T_SPG5, P_ICL1-7DLH-T_PRM9, P_PCK1^SLS-T_CPS1	this work
pJM033	2μ yeast ori; URA3; ColE1 ori; AmpR; $P_{ADH2}\text{-IO-T}_{SPG5},$ $P_{ICL1}\text{-}7DLGT\text{-}T_{IDP1},$ $P_{MLS1}\text{-}Lj7DLH\text{-}T_{PRM9}$	this work
pJM034	2μ yeast ori; URA3; ColE1 ori; AmpR; P_ADH2-IO-T_SPG5, P_ICL1-7DLGT-T_IDP1, P_MLS1-Rs7DLH-T_PRM9	this work
pJM035	2μ yeast ori; URA3; ColE1 ori; AmpR; P_ADH2-IO-T_SPG5, P_ICL1-7DLGT-T_IDP1, P_MLS1-T117-7DLH-T_PRM9	this work
pJM036	2μ yeast ori; URA3; ColE1 ori; AmpR; P_ADH2-IO-T_SPG5, P_ICL1-7DLGT-T_IDP1, P_MLS1-Ti18-7DLH-T_PRM9	this work
pJM037	2μ yeast ori; URA3; ColE1 ori; AmpR; P $_{\rm ADH2}$ -IO- $T_{\rm SPG5}$, P $_{\rm ICLI}$ -7DLGT- $T_{\rm IDPI}$, P $_{\rm MLS1}$ -Ug7DLH- $T_{\rm PRM9}$	this work
pJM057	CEN/ARS yeast ori; HIS3; ColE1 ori; AmpR; P_{ADH2} -IO- T_{SPG5} , P_{ICL1} -7DLH- T_{PRM9} , P_{PCK1} -SLS- T_{CPS1}	this work
pJM061	CEN/ARS yeast ori; HIS3; ColE1 ori; AmpR; P_{ADH2} -IO- T_{SPG5}	this work
pJM062	CEN/ARS yeast ori; HIS3; ColE1 ori; AmpR; $P_{ICLI-7DLH-T_{PRM9}}$	this work
pJM063	CEN/ARS yeast ori; HIS3; ColE1 ori; AmpR; P_{PCK1} -SLS- T_{CPS1}	this work
pJM064	2μ yeast ori; URA3; ColE1 ori; AmpR; P $_{\rm ADH2}$ -IO- $T_{\rm SPG5}$, P $_{\rm ICL1}$ -7DLH- $T_{\rm PRM9}$	this work
pJM065	2μ yeast ori; URA3; ColE1 ori; AmpR; P $_{\rm ADH2}$ -IO- $T_{\rm SPG5}$, P $_{\rm PCK1}$ -SLS- $T_{\rm CPS1}$	this work
pJM066	2μ yeast ori; URA3; ColE1 ori; AmpR; $P_{ICL1}\text{-}7DLH-T_{PRM9},\ P_{PCK1}\text{-}SLS\text{-}T_{CPS1}$	this work

to the α,β -unsaturated carboxylic acid. Coexpression of IO and 7DLGT, however, led to formation of 7-deoxyloganic acid as confirmed by comparison to an authentic standard (Figure 2B). This confirms that the glucosylation of the hemiacetal is protective and enables assessment of IO activities through

ACS Synthetic Biology pubs.acs.org/synthbio Research Article

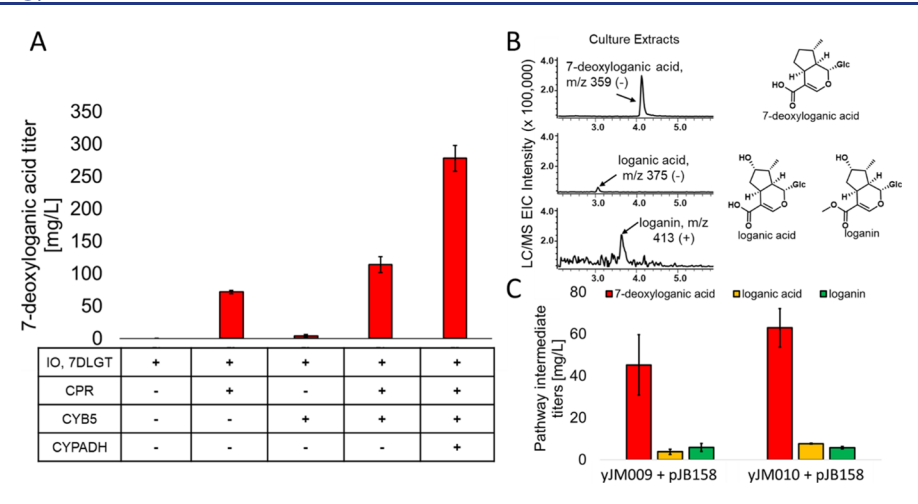


Figure 2. Optimizing expression of pathway accessory enzymes. (A) 7-Deoxyloganic acid production titers between strains expressing plasmids harboring different combinations of accessory enzymes; (B) extracted ion chromatograms of pathway intermediates of their characteristic m/z signals from LC/MS and their structures. The retention times match the standards; (C) production titers of 7-deoxyloganic acid, loganic acid, and loganin in yJM009 and yJM010 cotransformed with pJB152 and pJB040. Bars indicate the mean of biological triplicates with the error bars representing the standard error.

quantification of 7-deoxyloganic acid by liquid chromatography/mass spectrometry (LC/MS).

The strain yJB051 was transformed with a high-copy (2µ origin of replication) plasmid (pJB152, Table 1) encoding IO and 7DLGT under the control of ADH2p and ICL1p, respectively. Separate 2μ vectors containing either CPR, CYB5, CPR/CYB5, or CPR/CYB5/CYPADH under ADH2like auto-inducible promoters were cotransformed (pJB154, pJB155, pJB156, or pJB041, Table 1). Twenty-four hours after outgrowth of the yeast transformants, the cells were inoculated in yeast extract peptone dextrose (YPD)-rich media. Nepetalactol dissolved in ethanol was added to a concentration of 336.5 mg/L to each culture and allowed to grow for a further 24 h. The cultures were then extracted and analyzed by LC/MS for 7-deoxyloganic acid titers (Figure 2A). No production of 7-deoxyloganic acid was detected when the accessory enzymes were excluded, confirming that endogenous yeast redox partner enzymes are not compatible with IO (Figure 2A). Expression of CPR alone resulted in a 7deoxyloganic acid titer of 71.7 ± 2.5 mg/L, while expression of CYB5 alone resulted in a much lower titer of 3.9 \pm 2.3 mg/L. When CPR and CYB5 were expressed together, we observed a titer of 114.0 \pm 12.5 mg/L. These results indicate that CPR is the major electron donor to IO and can synergize with CYB5 to give the highest conversion. This is consistent with results from other researchers working with plant P450s. 10,39 When CYPADH was coexpressed, we observed a 2.5-fold increase in the 7-deoxyloganic acid titer to 278.0 \pm 19.8 mg/L, in agreement with its ancillary role in the oxidation of nepetalactol.11

Based on these results, we next integrated a cassette encoding the accessory enzymes under the regulation of ADH2-like promoters into yJB051 at the OYE3 locus to generate strain yJM009 (Table 1). This genomic site was selected based on RNA-Seq analysis that the OYE3 locus is upregulated in the presence of the early strictosidine pathway terpene intermediates (data not shown). We hypothesized that upon addition of terpene substrate, the OYE3 locus becomes more accessible to transcriptional machinery and allows for stronger transcription. This strain was transformed with the 2μ plasmid pJB158 expressing four downstream enzymes from

nepetalactol, IO, 7DLGT, 7DLH, and LAMT, each under auto-inducible promoters (pJB158, Table 1). Upon feeding nepetalactol to a concentration of 336.5 mg/L and further incubation for 24 h, the metabolites were extracted and analyzed. We detected emergence of three expected pathway intermediates, 7-deoxyloganic acid (45.2 \pm 14.4 mg/L), loganic acid (3.8 \pm 1.3 mg/L), and loganin (5.9 \pm 1.8 mg/L), based on comparison of mass and retention times to authentic standards (Figures 2B,C, S11, and S12).

While auto-inducible promoters were selected for expression of the biosynthetic enzymes, constitutive expression of CPR/ CYB5/CYPADH to accumulate these accessory enzymes prior to P450 enzyme expression may lead to enhanced substrate turnover. To examine this possibility, we next constructed the strain yJM010. This strain contains CPR, CYB5, and CYPADH under the constitutive promoters TEF1p, PGK1p, and TDH3p, respectively. These promoters were selected as they each exhibit moderate constitutive expression levels. The strain yJM010 was transformed with pJB158 and fed nepetalactol 24 h after inoculation into rich media, the time point at which expression of the pathway enzymes under the ADH2-like promoters is maximized. Following metabolite extraction and analysis, pathway intermediates were quantified to 63.0 ± 4.5 mg/L of 7-deoxyloganic acid, 7.7 ± 1.0 mg/L of loganic acid, and 5.8 ± 0.4 mg/L of loganin (Figure 2C). While the loganin titer in yJM010 was similar to that of yJM009 (5.9 \pm 1.8 and 5.8 ± 0.4 mg/L, respectively), 7-deoxyloganic acid and loganic acid titers were higher in yJM010, indicating an overall increase in total downstream pathway flux from the initial substrate nepetalactol. Based on these titer improvements, strain yJM010 was selected for further platform construction.

Bioprospecting of 7DLH Homologues Showed that Cr7DLH has the Highest Activity. As evident from the bioconversion of nepetalactol to loganic acid upon coexpression of IO, 7DLGT, 7DLH, and LAMT, 7-deoxyloganic acid, the product of 7DLGT, is the major product (Figure 2C). Quantifying the levels of metabolites extracted from intracellular and supernatant fractions revealed that >80% of 7-deoxyloganic acid accumulates in the culture supernatant (Figure S2). We reason that this could be due to the low activity of *C. roseus* 7DLH (Cr7DLH), which may result in

ACS Synthetic Biology pubs.acs.org/synthbio Research Article

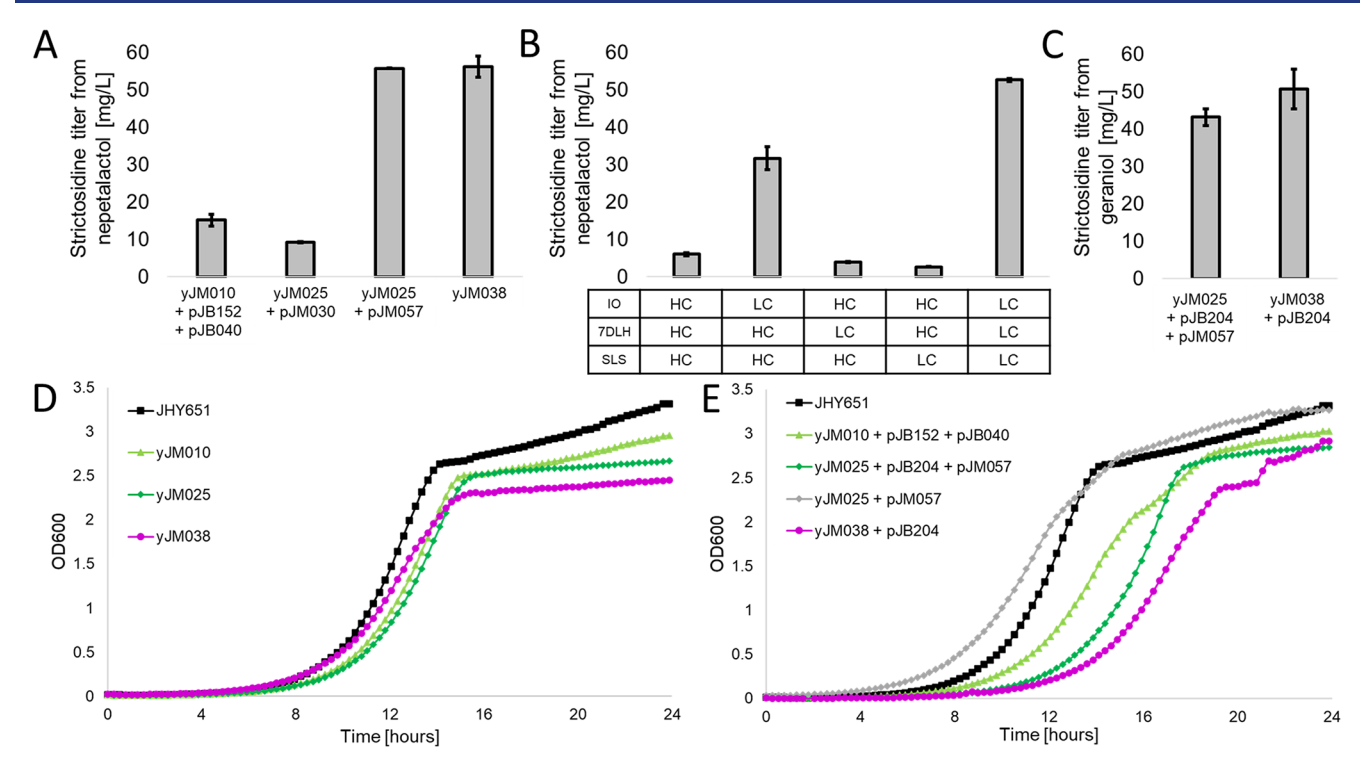


Figure 3. Comparison of strictosidine platforms. (A) Strictosidine titers of platform strains starting from nepetalactol; (B) strictosidine titers from varied copy numbers of plasmids expressing pathway P450s. HC: high-copy vector and LC: low-copy vector; (C) strictosidine titers of platform strains starting from geraniol; (D) growth curves of untransformed and plasmid-less strains compared against the wild-type; and (E) growth curves of transformed strictosidine production strains compared against the wild-type. Bars indicate the mean of biological triplicates with the error bars representing the standard error.

most of the substrate being transported to the extracellular space by yeast endogenous transporters. To potentially improve the activity of 7DLH, we replaced the Cr7DLH in the expression plasmid with a panel of seven putative 7DLH enzymes (pJM022-pJM023 and pJM033-pJM037, Table 1) from several different plant families including Apocynaceae, Rubiaceae, Caprifoliaceae, and Nyssaceae (Figure S10). Sequence alignments indicate that all 7DLH homologue sequences contain a membrane anchor region at the Ntermini. Alignment of CPR sequences from these species showed high sequence identity to that of the C. roseus CPR (Figure S9). Metabolite analysis showed that four of the seven bioprospected 7DLHs supported loganin production (Figure S1). Based on loganin titers, Cr7DLH remained the one with the highest activity in yeast. 7DLH from L. japonica showed the next highest activity at ~82% activity relative to Cr7DLH, while 7DLH from R. serpentina and two 7DLH homologues from Catharanthus acuminata both showed less than 20% activity. The 7DLH homologues from T. iboga and U. guianensis did not support any synthesis of loganin in yeast, as only 7-deoxyloganic acid is detected. As a result, Cr7DLH (referred to as 7DLH) was used in all subsequent studies.

Biosynthesis of Strictosidine from Nepetalactol. Following optimization of the P450 partner enzymes, we introduced the remaining biosynthetic genes in the strictosidine pathway to establish a baseline of strictosidine production from nepetalactol. The strain yJM010 was transformed with 2μ vectors, pJB152 expressing IO, 7DLGT, 7DLH, and LAMT, and pJB040 expressing SLS and STR. All genes are under the control of ADH2-like promoters (Table 1). After strain outgrowth, nepetalactol and tryptamine both dissolved in ethanol were supplied to concentrations of 336.5 and 320.4

mg/L and the strains were further grown for 24 h. LC/MS analysis of extracts showed the emergence of a new compound with m/z=531. The compound was compared with an authentic standard of strictosidine obtained via chemical synthesis, ¹⁵ which showed identical retention time and MS/MS fragmentation patterns (Figure S4). Using the authentic strictosidine to establish a standard curve, the titer from the yeast pathway was measured to be 15.2 ± 1.6 mg/L between biological triplicates (Figures 3A and S13). In this strain, pathway intermediates 7-deoxyloganic acid, loganic acid, and loganin accumulated to titers of 43.9 ± 3.1 , 5.2 ± 0.4 , and 3.1 ± 0.6 mg/L, respectively. The molar ratios of these intermediates with respect to each other were consistent with previous strains.

Further host optimization studies were performed starting from yJM010. From the measurement of pathway intermediates during the fed-batch biotransformation, we noted the non-P450 enzymes, 7DLGT, LAMT, and STR, were not rate-limiting. Thus, a single cassette of genes encoding these three enzymes under ADH2-like promoters was integrated into the YPCRCTy1-2 locus to give the yeast strain yJM025. This strain was then transformed with a 2μ vector pJM030 containing the genes encoding the P450s IO, 7DLH, and SLS under ADH2-like promoters (Table 1). Feeding nepetalactol and tryptamine to this strain resulted in a slight decrease of the strictosidine titer to 9.2 \pm 0.1 mg/L (Figure 3A).

Tuning P450 Gene Copy Numbers. Because most plant P450 enzymes are translocated to the endoplasmic reticulum (ER), overexpression of these enzymes can disrupt yeast endomembrane homeostasis and activate the unfolded protein response pathway, resulting in degradation of the exogenous

ACS Synthetic Biology pubs.acs.org/synthbio Research Article

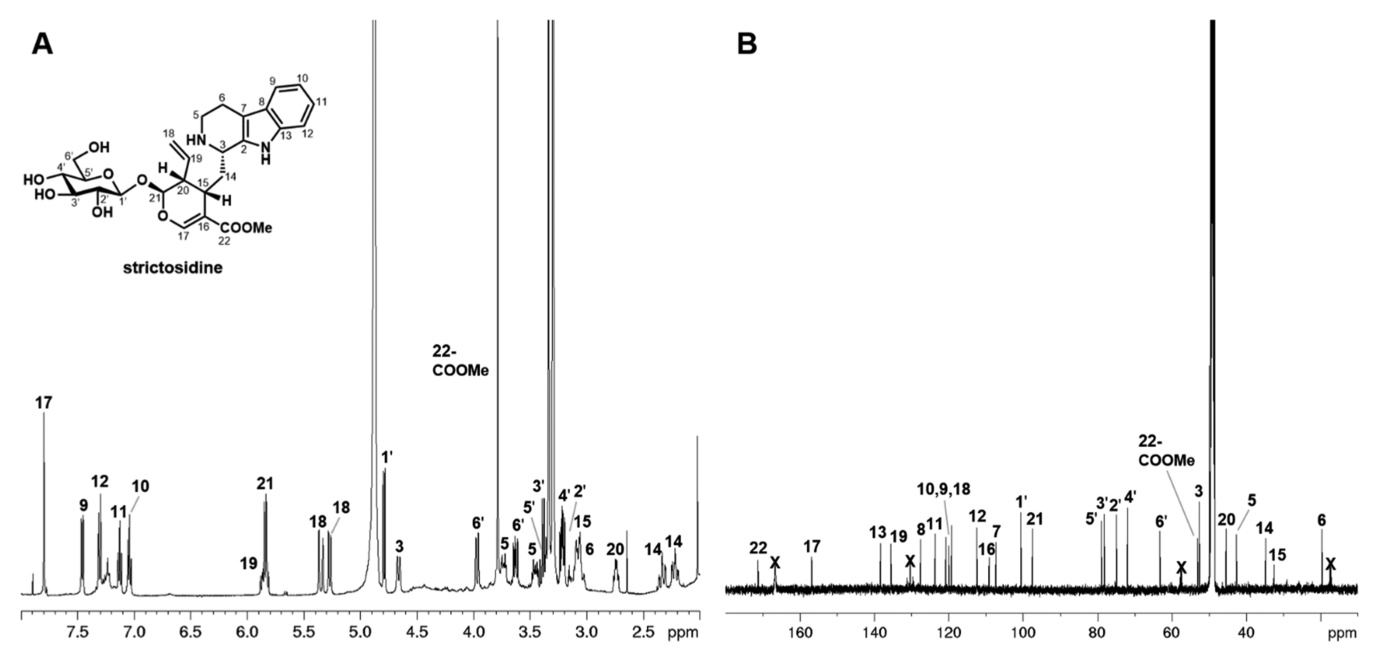


Figure 4. NMR spectra of purified strictosidine from yeast. (A) 1 H NMR at 500 MHz in methanol- d_4 ; (B) 13 C NMR at 125 MHz in methanol- d_4 . Strictosidine is purified in the salt form as a result of acidic chromatographic conditions. For detailed assignment of peaks, see Table S2 and Figures S5–S7.

protein. He effect of P450 expression levels (high copy vs low copy) on product titer, however, varies with different pathways. High-copy (2μ) and low-copy (CEN/ARS) expression vectors containing the pathway P450s (IO, 7DLH, and SLS) were compared to evaluate changes in the strictosidine titer. The 2μ origin of replication of pJM030 was swapped with a CEN/ARS sequence to generate plasmid pJM057 (Table 1). The low-copy pJM057 was then transformed into yJM025, and the resulting titer was measured. Remarkably, the strictosidine titer was significantly elevated to 55.8 ± 0.1 mg/L upon feeding 336.5 mg/L of nepetalactol and 320.4 mg/L of tryptamine (Figure 3A). There was a corresponding decrease in pathway intermediates to 36.0 ± 3.7 , 9.4 ± 0.5 , and 0.9 ± 0.3 mg/L for 7-deoxyloganic acid, loganic acid, and loganin, respectively (Figure S3).

To evaluate if altering the expression level of any one of the three P450 enzymes was responsible for the significant increase in the titer, we generated plasmid pairs that contain each pathway P450 on a low-copy vector, with the other two on a high-copy vector (pJM061 + pJM066, pJM062 + pJM065, pJM063 + pJM064, Table 1). Every plasmid pair was cotransformed into yJM025, and the resulting yeast strain was assayed quantitatively for strictosidine formation (Figure 3B). From these results, decreasing the copy number of the gene encoding IO alone resulted in the greatest improvement to the strictosidine titer from 9.2 \pm 0.1 to 34.8 \pm 1.1 mg/L. Several possibilities may contribute to the significant increase in the titer. First, sequence analysis of IO showed that the protein has two annotated transmembrane domains, compared with 7DLH and SLS, each having only one, which suggests that IO may disrupt the ER membrane to a greater extent during translocation. Decreasing the copy number may therefore alleviate such ER disturbances. Second, as noted earlier, the product of IO, 7-deoxyloganetic acid, is unstable, which may lead to rapid degradation if the relative activity of IO is higher compared to downstream enzyme 7DLGT.

While expressing 7DLH or SLS on low-copy plasmid did not significantly affect the titer of strictosidine, it is evident that collectively placing all three P450s on low copy vectors had the most improvement (Figure 3B). Based on this finding, a cassette encoding all three P450s under auto-inducible promoters was integrated into the HIS3 locus of yJM025 to afford yJM038 (Table 1). The plasmid-free strain yJM038 produced 56.2 ± 2.8 mg/L of strictosidine from 336.5 mg/L of nepetalactol and 320.4 mg/L tryptamine 24 h after feeding (Figure 3A).

Biosynthesis of Strictosidine from Geraniol. Given the success of nepetalactol to strictosidine biotransformation in yJM038, we next tested conversion starting from the commodity chemical geraniol. The discovery of the major latex protein-like cyclase, MLPL, from Nepeta mussinii²³ completes the early pathway from geraniol to nepetalactol and decreases shunt product formation after ISY reduction (Figure 1).44 To demonstrate that geraniol can serve as a precursor, strain yJM025 was co-transformed with the CEN/ ARS plasmid pJM057 expressing IO, 7DLH, and SLS; and 2μ plasmid pJB204 expressing G8H, GOR, ISY, and MLPL (Table 1). All genes are under the control of ADH2 and ADH2-like promoters. Fed-batch assays of this transformed strain were fed to a concentration of 308.5 mg/L geraniol and 320.4 mg/L of tryptamine resulting in a strictosidine titer of 43.2 ± 2.3 mg/L (Figure 3C), a comparable titer to starting from nepetalactol. Interestingly, no pathway intermediates were detected in this strain. Entering the pathway at geraniol likely results in a steadier flux of intermediates through the pathway (especially at the IO step) and reduces accumulation at bottleneck steps like 7DLGT and 7DLH. Then, yJM038 transformed with pJB204 produced 50.7 ± 5.3 mg/L of strictosidine from geraniol and tryptamine (Figure 3C). In previously developed strictosidine-producing strains, the P450 G8H was identified as a major pathway bottleneck, precluding the use of geraniol as a feedstock.¹¹ The tuning of the P450 accessory enzyme and elimination of shunt pathways in

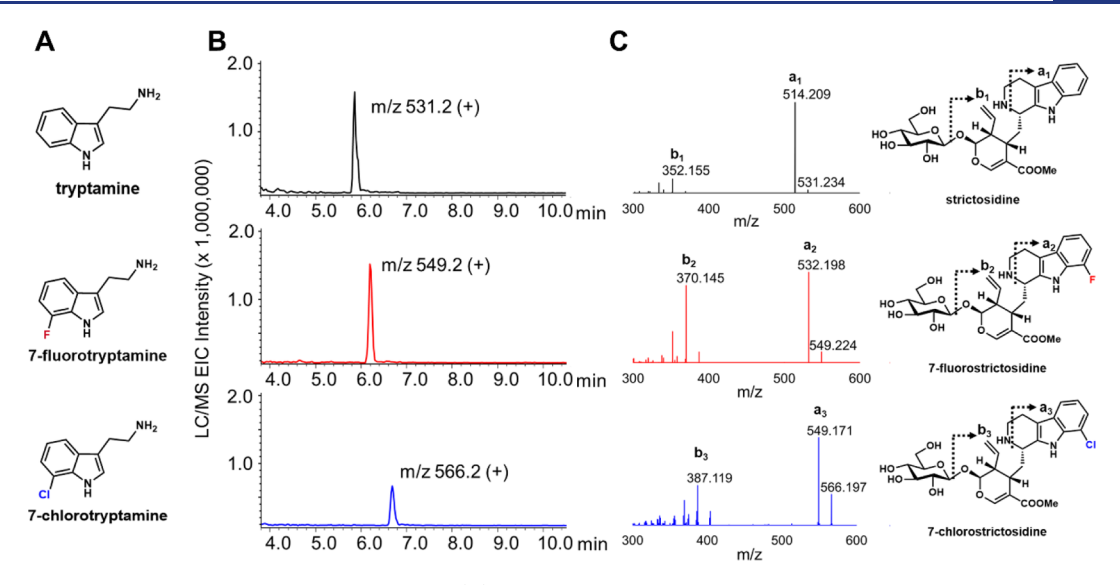


Figure 5. Production of halogenated strictosidine derivatives. (A) Structures of tryptamines successfully incorporated into strictosidine *in vivo*; (B) extracted ion chromatogram of characteristic m/z [M + H]⁺ signal for different strictosidine analogues from LC/MS analysis; (C) tandem mass spectrometry (MS/MS) fragmentation patterns from QTOF-LC/MS for strictosidine (black), 7-fluorostrictosidine (red), and 7-chlorostrictosidine (blue) and corresponding predominant product ion structures.

combination with MLPL resulted in robust metabolic flux through the early seco-iridoid pathway to nepetalactol. Hence, strictosidine can be produced at a comparable titer starting from geraniol, a considerably cheaper precursor compared to nepetalactol, using a single plasmid-carrying yeast host.

Purification and Characterization of Strictosidine from Yeast. To fully characterize the strictosidine produced from the strain, we scaled up (1 L) the geraniol-based production using yJM025 co-transformed with pJB204 and pJM057. The produced strictosidine was purified to homogeneity for NMR characterization. This would confirm the identity of microbial strictosidine and demonstrate feasibility in obtaining the pure compound in meaningful quantities. The yeast supernatant underwent several stages of column chromatography to arrive at fractions enriched with strictosidine. These fractions underwent final purification using semipreparative high-performance liquid chromatography (HPLC). Purified strictosidine, a yellow amorphous solid, was then analyzed by proton nuclear magnetic resonance (¹H NMR), carbon nuclear magnetic resonance (¹³C NMR) (Figure 4), and two-dimensional NMR (Figures S5-S8). These spectra were matched to data obtained from a synthetic standard (Table S2). A nuclear overhauser effect spectroscopy experiment showed an interaction between H-3 and H-15, supporting that the strictosidine produced was the correct C3 epimer (Figure S8). Isolation of strictosidine in its pure form from yeast was made possible with the high-titer strain and underscores the usefulness of this platform in investigating downstream MIA pathways.

Yeast Strains Retain Robust Growth with Pathway Reconstitution. The growth rates of the engineered strains were quantitatively compared to the starting JHY651 strain to assess the impact of the modifications to yeast robustness. Both untransformed strains and plasmid-transformed strains were assayed. For the untransformed strains, the growth rates slightly decreased as more genes were integrated into the genome, as expected from the increased metabolic load (Figure 3D). However, the impact on overall cell growth was minimal with similar stationary phase OD₆₀₀ values. In the single-

double-transformed yeast strains used in production of pathway intermediates and strictosidine, cellular growth rates were impaired more significantly, with a longer lag phase and a slower exponential phase (Figure 3E). However, by approximately 16 h after inoculation, most strains had grown to a similar cell density as JHY651. The ability for all engineered strains to reach a similar cell density as JHY651 after about 24 h highlights the usefulness of the auto-inducible promoter system to decouple the growth and production phases of yeast despite the expression of 13 heterologous enzymes.

Biosynthesis of Halogenated Strictosidine Through Feeding Modified Tryptamines. Using the strictosidine producing yeast strain constructed as mentioned above, we next tested the ability of the strain to produce analogues of strictosidine through precursor-directed biosynthesis. In particular, STR was shown to have relaxed substrate specificity toward substituted tryptamine analogues. Because no strictosidine production can be detected without supplementing tryptamine, feeding substituted tryptamines would lead to the biosynthesis of modified strictosidine analogues with minimal background. A similar strategy was recently demonstrated by Li *et al.* to generate modified noscapine analogues from substituted tyrosines.

A panel of five substituted tryptamines (5-bromotryptamine, 6-methoxytryptamine, 6-chlorotryptamine, 7-chlorotrypamine, and 7-fluorotryptamine) along with geraniol were fed into separate yJM025 cultures co-transformed with pJM057 and pJB204. We observed no growth defects between strains following feeding compared to the unmodified tryptamine control. Twenty-four hours after feeding, cultures were extracted with acetone and ran on OTOF-LC/MS for analysis. The chromatographs were filtered for the expected masses of the modified strictosidine products. New compounds were detected upon 7-fluorotryptamine and 7-chlorotryptamine supplementation (Figure 5). The retention time shifts of the compounds are consistent with halogen incorporations. MS/ MS analysis of the strictosidine analogues further suggested that these signals correspond to halogenated strictosidine analogues (Figure 5B). The differences between the 7fluorostrictosidine and strictosidine parent ion (549.224 vs 531.234, respectively) and major daughter ions (532.198 and 370.145 vs 514.209 and 352.155, respectively) are 17.99 mass units, corresponding to a replacement of a hydrogen with a fluorine atom. Similarly, the differences in masses of parent and daughter ions between 7-chlorostrictosidine and strictosidine (566.197, 549.171, and 387.119 vs 531.234, 514.209, and 352.155, respectively) are 34.96 mass units, corresponding to the replacement of a hydrogen with a chlorine atom. The lack of incorporation of other tryptamine analogues is consistent with previous reports which stated that STR does not tolerate 5- and 6-substituted tryptamines well.⁴⁸ Point mutations that result in a larger binding pocket of STR have been identified.⁴⁶ Recapitulation of these mutations in the STR gene may expand the scope of the modified strictosidine analogues obtainable from yeast-based precursor-directed biosynthesis.

CONCLUSIONS

We have engineered a yeast strain capable of producing ~ 50 mg/L of strictosidine from geraniol. This was achieved by optimizing the expression of P450s and P450 accessory enzymes, decoupling the growth and production stages using auto-inducible promoters, and entering the pathway at high initial concentrations of commodity precursors. Our strain improvements resulted in scalable titers that enabled the isolation of purified strictosidine. We have also demonstrated that our platform can be leveraged for the production of strictosidine analogues by feeding modified tryptamines. Moreover, our engineered host retains robust strain health, a key factor in strain development for lengthy MIA pathways. Thus, our high-titer strictosidine-producing host enables the development of microbial production of an expansive class of therapeutic plant natural products.

METHODS

Plasmid and Strain Construction. All yeast expression plasmids were cloned using yeast homologous recombination. Fragments for recombination were amplified using Q5 polymerase (NEB) with ~35 bp of homology overlap to subsequent fragments and column purified using a Zymoclean Gel DNA Recovery Kit (Zymo Research). Strictosidine pathway genes from C. roseus and putative 7DLHs were codon-optimized and synthesized by Gen9 or IDT (Table S1). The auto-inducible ADH2 and ADH2-like promoters and high-capacity terminators were amplified from S. cerevisiae genomic DNA. Amplified fragments for cloning were transformed into yeast using the standard lithium acetate method,⁴⁹ plated onto the corresponding supplemental complete media (SC) deficient for uracil, leucine, and/or histidine. After 48 hours of outgrowth, the plasmid was extracted from clumps of colonies using a Zymoprep Yeast Plasmid Miniprep I kit (Zymo Research). The yeast miniprep solution was then transformed into electrocompetent TOP10 Escherichia coli cells for plasmid propagation using electroporation and plated onto LB agar supplemented with 100 mg/L carbenicillin. Several colonies after 16 h of outgrowth were inoculated into liquid media supplemented with carbenicillin, grown overnight, and miniprepped using a Zyppy Plasmid Miniprep Kit (Zymo Research). Successful plasmid constructs were identified through restriction digest (NEB) and then verified by Sanger sequencing (Laragen). Genomic integration of expression cassettes was achieved through a two-stage strategy. A LEU2

marker was first integrated at the genomic loci of choice using a linearized donor DNA from a plasmid containing 300-500 bp of homology flanking the LEU2 marker, following the standard transformation protocol as described above. Next, the linearized expression cassette of choice with 300-500 bp of homology from a homology donor plasmid was co-transformed with a plasmid containing a CRISPR-Cas9 system⁵⁰ encoding an sgRNA targeting the LEU2 marker. The transformed yeast was then inoculated into 3 mL of YPD media for outgrowth for 14 h and then 200 μ L was plated onto YPD agar plates supplemented with 400 mg/L G418 sulfate. After 48 hours of growth, colonies were first screened by counter selection on SC agar plates deficient for leucine and then by colony PCR. Successful integrations were subject to further characterization and verification by genomic DNA extraction using a YeaStar Genomic DNA Kit (Zymo Research) and subsequent PCR and Sanger sequencing.

Culture and Fed-Batch Assay Conditions. For all yeast assays, single colonies were picked and inoculated into 500 μ L of the respective SC media deficient of uracil, leucine, and/or histidine and grown overnight in a Lab-Therm LX-T (Adolf Kuhner) incubator shaker at 280 RPM and 28 °C. This seed culture was then inoculated into 500 μ L YPD in a 96 deep-well plate or 1.5 mL YPD in culture tube to an OD₆₀₀ of 0.1. 96 deep-well plate cultures are covered with AeraSeal film (Excel Scientific) and grown at 28 °C, shaking at 400 RPM. 1.5 mL cultures are grown at 28 °C and shaken at 280 RPM. After 24 hours of outgrowth in rich media, strains were fed geraniol or nepetalactol and tryptamine from 200 mM stocks dissolved in ethanol to a culture concentration of 2 mM.

Growth Assays. All strains were grown overnight in biological triplicate in 1 mL YPD or respective selective media. These overnight cultures were used to inoculate 100 μ L of YPD to a starting OD₆₀₀ of 0.01 in a 96-well clear plate. The plate was then sealed and placed into an Infinite M200 plate reader (TECAN) for incubation. Cultures were continuously shaken at 280 RPM at 28 °C with OD₆₀₀ measurements taken every 15 min for 24 h.

Strictosidine and Pathway Intermediate Extraction and Analysis. Samples were extracted 24 h after feeding substrates. 200 μ L of whole culture was extracted with 200 μ L acetone and vortexed for 30 s. The samples were then centrifuged for 10 min at maximum speed. The supernatant is then removed and placed into a clean tube, and an equal volume of MilliQ water is added to dilute the sample. Samples were then analyzed on a Shimadzu 2020 EV LC/MS equipped with a Phenomenex Kinetex C18, 1.7 μ m, 100 Å, 2.1 × 100 mm reverse-phase column. Both positive- and negative-mode electrospray ionization were performed with a linear gradient of 5-95% acetonitrile-H₂O spiked with 0.1% formic acid over 15 min and then 95% acetonitrile for 3 min with a flow rate of 0.3 mL/min. High-resolution MS/MS data was collected on an Agilent 6545 LC/Q-TOF MS with a 25 V collision voltage. Strictosidine and pathway intermediate peaks were verified by comparison to available standards and quantified using calibration curves generated from standards. 7-Deoxyloganic acid was quantified using loganic acid as a proxy for LC/MS mass response because sufficient quantities of the standard were not able to be obtained. Loganic acid and loganin standards were purchased from ChemFaces. Strictosidine standard was a gift from Neil Garg's lab, UCLA.

Strictosidine Purification. Yeast strain yJM025 cotransformed with pJB204 and pJM057 used for the production

of strictosidine at a 1 L scale. Following outgrowth, geraniol and tryptamine in ethanol were added to a concentration of 2 mM each. 24 hours after feeding, the culture was centrifuged to separate the cell pellet and culture supernatant. The supernatant was subjected to HP-20 column chromatography (water to MeOH). The MeOH eluate fraction was applied to a Sephadex LH-20 column (MeOH) to give three fractions (frs. 1-3). Fr. 2 was subjected to ODS MPLC and carried out on a RediSep Gold Reverse-phase C18 column (TELEDYNE, Lincoln, USA), (MeOH/ H_2O , 0:100 \rightarrow 100:0) to give six fractions (frs. 2.1-2.6), and then fr. 2.5 was further separated by Sephadex LH-20 column chromatography (CHCl₃/MeOH, 5:5) to obtain three fractions (frs. 2.5.1-2.5.3). Fr. 2.5.2 was purified by ODS HPLC on a COSMOSIL 5C18-AR-II $column(\varphi 10 \times 250 \text{ mm}, MeCN/H₂O/formic acid,$ 20:80:0.1) to furnish strictosidine. The 1D NMR spectrum was obtained on a Bruker AV500 spectrometer for structure verifications and compared with a standard from Neil Garg's lab, UCLA. The resonances of residual methanol ($\delta_{\rm H}$ 3.30 and $\delta_{\rm C}$ 49.0) were used as internal references for the ¹H and ¹³C NMR spectra. High-resolution MS/MS data were collected on an Agilent 6545 LC/Q-TOF MS with a collision voltage of 25.

ASSOCIATED CONTENT

Supporting Information

The Supporting Information is available free of charge at https://pubs.acs.org/doi/10.1021/acssynbio.2c00037.

Gene sequences, NMR spectroscopic data, additional assays, MS/MS spectra, sequence alignments, and standard curves (PDF)

AUTHOR INFORMATION

Corresponding Author

Yi Tang — Department of Chemical and Biomolecular Engineering and Department of Chemistry and Biochemistry, University of California, Los Angeles, California 90095, United States; orcid.org/0000-0003-1597-0141; Email: yitang@ucla.edu

Authors

Joshua Misa — Department of Chemical and Biomolecular Engineering, University of California, Los Angeles, California 90095, United States; orcid.org/0000-0002-3722-8573

John M. Billingsley – Department of Chemical and Biomolecular Engineering, University of California, Los Angeles, California 90095, United States; ⊚ orcid.org/ 0000-0001-9300-9378

Kanji Niwa – Department of Chemical and Biomolecular Engineering, University of California, Los Angeles, California 90095, United States

Rachel K. Yu – Department of Chemical and Biomolecular Engineering, University of California, Los Angeles, California 90095, United States

Complete contact information is available at: https://pubs.acs.org/10.1021/acssynbio.2c00037

Author Contributions

J.M., J.M.B., and Y.T. conceived the project, designed the experiments, and wrote the manuscript. J.M., J.M.B., K.N., and R.K.Y. performed the experiments. All authors contributed to data analysis and revision of the manuscript.

Notes

The authors declare no competing financial interest.

ACKNOWLEDGMENTS

This work was supported by the NIH 1R01AT010001. J.M. was supported by NIH NIGMS-funded predoctoral fellowship, T32GM136614, and is a summer fellow of the BioPacific Program supported by the NSF cooperative agreement (DMR-1933487). We thank Prof. Sarah O'Connor for helpful discussions and gene sequences and Prof. Neil Garg for providing a strictosidine standard. We also thank Danielle Yee for helpful discussions and technical assistance.

REFERENCES

- (1) Cravens, A.; Payne, J.; Smolke, C. D. Synthetic Biology Strategies for Microbial Biosynthesis of Plant Natural Products. *Nat. Commun.* **2019**, *10*, 2142–2153.
- (2) Pham, J. V.; Yilma, M. A.; Feliz, A.; Majid, M. T.; Maffetone, N.; Walker, J. R.; Kim, E.; Cho, H. J.; Reynolds, J. M.; Song, M. C.; Park, S. R.; Yoon, Y. J. A Review of the Microbial Production of Bioactive Natural Products and Biologics. *Front. Microbiol.* **2019**, *10*, 1404.
- (3) Jamieson, C. S.; Misa, J.; Tang, Y.; Billingsley, J. M. Biosynthesis and Synthetic Biology of Psychoactive Natural Products. *Chem. Soc. Rev.* **2021**, *50*, 6950–7008.
- (4) Kavšček, M.; Stražar, M.; Curk, T.; Natter, K.; Petrovič, U. Yeast as a Cell Factory: Current State and Perspectives. *Microb. Cell Fact.* **2015**. *14*. 94.
- (5) Day, K. J.; Casler, J. C.; Glick, B. S. Budding Yeast Has a Minimal Endomembrane System. *Dev. Cell* **2018**, 44, 56–72.e4.
- (6) Zhang, X.; Li, S. Expansion of Chemical Space for Natural Products by Uncommon P450 Reactions. *Nat. Prod. Rep.* **2017**, *34*, 1061–1089.
- (7) Srinivasan, P.; Smolke, C. D. Biosynthesis of Medicinal Tropane Alkaloids in Yeast. *Nat* **2020**, *585*, 614–619.
- (8) Galanie, S.; Thodey, K.; Trenchard, I. J.; Filsinger Interrante, M.; Smolke, C. D. Complete Biosynthesis of Opioids in Yeast. *Science* **2015**, *349*, 1095–1100.
- (9) Li, Y.; Li, S.; Thodey, K.; Trenchard, I.; Cravens, A.; Smolke, C. D. Complete Biosynthesis of Noscapine and Halogenated Alkaloids in Yeast. *Proc. Natl. Acad. Sci. U.S.A.* **2018**, *115*, E3922–E3931.
- (10) Paddon, C. J.; Westfall, P. J.; Pitera, D. J.; Benjamin, K.; Fisher, K.; McPhee, D.; Leavell, M. D.; Tai, A.; Main, A.; Eng, D.; Polichuk, D. R.; Teoh, K. H.; Reed, D. W.; Treynor, T.; Lenihan, J.; Jiang, H.; Fleck, M.; Bajad, S.; Dang, G.; Dengrove, D.; Diola, D.; Dorin, G.; Ellens, K. W.; Fickes, S.; Galazzo, J.; Gaucher, S. P.; Geistlinger, T.; Henry, R.; Hepp, M.; Horning, T.; Iqbal, T.; Kizer, L.; Lieu, B.; Melis, D.; Moss, N.; Regentin, R.; Secrest, S.; Tsuruta, H.; Vazquez, R.; Westblade, L. F.; Xu, L.; Yu, M.; Zhang, Y.; Zhao, L.; Lievense, J.; Covello, P. S.; Keasling, J. D.; Reiling, K. K.; Renninger, N. S.; Newman, J. D. High-Level Semi-Synthetic Production of the Potent Antimalarial Artemisinin. *Nature* 2013, 496, 528–532.
- (11) Brown, S.; Clastre, M.; Courdavault, V.; O'Connor, S. E. De Novo Production of the Plant-Derived Alkaloid Strictosidine in Yeast. *Proc. Natl. Acad. Sci. U.S.A.* **2015**, *112*, 3205–3210.
- (12) O'Connor, S. E.; Maresh, J. J. Chemistry and Biology of Monoterpene Indole Alkaloid Biosynthesis. *Nat. Prod. Rep.* **2006**, 23, 532.
- (13) Rakumitsu, K.; Sakamoto, J.; Ishikawa, H. Total Syntheses of (—)-Secologanin, (—)-5-Carboxystrictosidine, and (—)-Rubenine. *Chem.—Eur. J.* **2019**, 25, 8996—9000.
- (14) Sakamoto, J.; Umeda, Y.; Rakumitsu, K.; Sumimoto, M.; Ishikawa, H. Total Syntheses of (–)-Strictosidine and Related Indole Alkaloid Glycosides. *Angew. Chem., Int. Ed.* **2020**, *59*, 13414–13422.
- (15) Anthony, S. M.; Tona, V.; Zou, Y.; Morrill, L. A.; Billingsley, J. M.; Lim, M.; Tang, Y.; Houk, K. N.; Garg, N. K. Total Synthesis of (–)-Strictosidine and Interception of Aryne Natural Product

- Derivatives "Strictosidyne" and "Strictosamidyne. J. Am. Chem. Soc. 2021, 143, 7471–7479.
- (16) Geerlings, A.; Redondo, F. J.; Contin, A.; Memelink, J.; Van der Heijden, R.; Verpoorte, R. Biotransformation of Tryptamine and Secologanin into Plant Terpenoid Indole Alkaloids by Transgenic Yeast. *Appl. Microbiol. Biotechnol.* **2001**, *56*, 420–424.
- (17) Nam, K. H.; Hwa, J. C.; Eo, J. J.; Mi, K. P.; Yong, H. Y.; Jang, R. L.; Jeong, H. P. In Vitro Biosynthesis of Strictosidine Usinglonicera Japonica Leaf Extracts and Recombinant Yeast. *J. Plant Biol.* **2007**, *50*, 315–320.
- (18) Iijima, Y.; Gang, D. R.; Fridman, E.; Lewinsohn, E.; Pichersky, E. Characterization of Geraniol Synthase from the Peltate Glands of Sweet Basil. *Plant Physiol.* **2004**, *134*, 370–379.
- (19) Collu, G.; Unver, N.; Peltenburg-Looman, A. M. G.; Van der Heijden, R.; Verpoorte, R.; Memelink, J. Geraniol 10-hydroxylase1, a cytochrome P450 enzyme involved in terpenoid indole alkaloid biosynthesis. *FEBS Lett.* **2001**, *508*, 215–220.
- (20) Geu-Flores, F.; Sherden, N. H.; Courdavault, V.; Burlat, V.; Glenn, W. S.; Wu, C.; Nims, E.; Cui, Y.; O'Connor, S. E. An Alternative Route to Cyclic Terpenes by Reductive Cyclization in Iridoid Biosynthesis. *Nature* **2012**, 492, 138–142.
- (21) Miettinen, K.; Dong, L.; Navrot, N.; Schneider, T.; Burlat, V.; Pollier, J.; Woittiez, L.; Van Der Krol, S.; Lugan, R.; Ilc, T.; Verpoorte, R.; Oksman-Caldentey, K.-M.; Martinoia, E.; Bouwmeester, H.; Goossens, A.; Memelink, J.; Werck-Reichhart, D. The Seco-Iridoid Pathway from Catharanthus Roseus. *Nat. Commun.* **2014**, *5*, 3606.
- (22) Lichman, B. R.; Kamileen, M. O.; Titchiner, G. R.; Saalbach, G.; Stevenson, C. E. M.; Lawson, D. M.; O'Connor, S. E. Uncoupled Activation and Cyclization in Catmint Reductive Terpenoid Biosynthesis. *Nat. Chem. Biol.* **2019**, *15*, 71–79.
- (23) Lichman, B. R.; Godden, G. T.; Hamilton, J. P.; Palmer, L.; Kamileen, M. O.; Zhao, D.; Vaillancourt, B.; Wood, J. C.; Sun, M.; Kinser, T. J.; Henry, L. K.; Rodriguez-Lopez, C.; Dudareva, N.; Soltis, D. E.; Soltis, P. S.; Buell, C. R.; O'Connor, S. E. The Evolutionary Origins of the Cat Attractant Nepetalactone in Catnip. *Sci. Adv.* **2020**, *6*, No. eaba0721.
- (24) Murata, J.; Roepke, J.; Gordon, H.; De Luca, V. The Leaf Epidermome of Catharanthus roseus Reveals Its Biochemical Specialization. *Plant Cell* **2008**, *20*, 524–542.
- (25) Irmler, S.; Schröder, G.; St-Pierre, B.; Crouch, N. P.; Hotze, M.; Schmidt, J.; Strack, D.; Matern, U.; Schröder, J. Indole Alkaloid Biosynthesis in Catharanthus Roseus: New Enzyme Activities and Identification of Cytochrome P450 CYP72A1 as Secologanin Synthase. *Plant J.* **2000**, *24*, 797–804.
- (26) Kutchan, T. M.; Hampp, N.; Lottspeich, F.; Beyreuther, K.; Zenk, M. H. The CDNA Clone for Strictosidine Synthase from Rauvolfia Serpentina DNA Sequence Determination and Expression in Escherichia Coli. *FEBS Lett.* **1988**, 237, 40–44.
- (27) Bracher, D.; Kutchan, T. M. Strictosidine Synthase from Rauvolfia Serpentina: Analysis of a Gene Involved in Indole Alkaloid Biosynthesis. *Arch. Biochem. Biophys.* **1992**, 294, 717–723.
- (28) Peng, B.; Williams, T. C.; Henry, M.; Nielsen, L. K.; Vickers, C. E. Controlling Heterologous Gene Expression in Yeast Cell Factories on Different Carbon Substrates and across the Diauxic Shift: A Comparison of Yeast Promoter Activities. *Microb. Cell Fact.* **2015**, *14*, 91
- (29) Yee, D. A.; DeNicola, A. B.; Billingsley, J. M.; Creso, J. G.; Subrahmanyam, V.; Tang, Y. Engineered Mitochondrial Production of Monoterpenes in Saccharomyces Cerevisiae. *Metab. Eng.* **2019**, *55*, 76–84
- (30) Zhao, J.; Li, C.; Zhang, Y.; Shen, Y.; Hou, J.; Bao, X. Dynamic Control of ERG20 Expression Combined with Minimized Endogenous Downstream Metabolism Contributes to the Improvement of Geraniol Production in Saccharomyces Cerevisiae. *Microb. Cell Fact.* 2017, 16, 17.
- (31) Liu, N.; Santala, S.; Stephanopoulos, G. Mixed Carbon Substrates: A Necessary Nuisance or a Missed Opportunity? *Curr. Opin. Biotechnol.* **2020**, *62*, 15.

- (32) Milne, N.; Thomsen, P.; Mølgaard Knudsen, N.; Rubaszka, P.; Kristensen, M.; Borodina, I. Metabolic Engineering of Saccharomyces Cerevisiae for the de Novo Production of Psilocybin and Related Tryptamine Derivatives. *Metab. Eng.* **2020**, *60*, 25–36.
- (33) Lee, K. M.; DaSilva, N. A. Evaluation of the Saccharomyces cerevisiae ADH2 promoter for protein synthesis. *Yeast* **2005**, 22, 431–440.
- (34) Harvey, C. J. B.; Tang, M.; Schlecht, U.; Horecka, J.; Fischer, C. R.; Lin, H. C.; Li, J.; Naughton, B.; Cherry, J.; Miranda, M.; Li, Y. F.; Chu, A. M.; Hennessy, J. R.; Vandova, G. A.; Inglis, D.; Aiyar, R. S.; Steinmetz, L. M.; Davis, R. W.; Medema, M. H.; Sattely, E.; Khosla, C.; St Onge, R. P.; Tang, Y.; Hillenmeyer, M. E. HEx: A Heterologous Expression Platform for the Discovery of Fungal Natural Products. *Sci. Adv.* **2018**, *4*, No. eaar5459.
- (35) Billingsley, J. M.; Denicola, A. B.; Barber, J. S.; Tang, M.-C.; Horecka, J.; Chu, A.; Garg, N. K.; Tang, Y. Engineering the Biocatalytic Selectivity of Iridoid Production in Saccharomyces Cerevisiae. *Metab. Eng.* **2017**, *44*, 117–125.
- (36) Smith, J. D.; Schlecht, U.; Xu, W.; Suresh, S.; Horecka, J.; Proctor, M. J.; Aiyar, R. S.; Bennett, R. A. O.; Chu, A.; Li, Y. F.; Roy, K.; Davis, R. W.; Steinmetz, L. M.; Hyman, R. W.; Levy, S. F.; St.Onge, R. P. A method for high-throughput production of sequence-verified DNA libraries and strain collections. *Mol. Syst. Biol.* **2017**, *13*, 913.
- (37) Ro, D.-K.; Paradise, E. M.; Ouellet, M.; Fisher, K. J.; Newman, K. L.; Ndungu, J. M.; Ho, K. A.; Eachus, R. A.; Ham, T. S.; Kirby, J.; Chang, M. C. Y.; Withers, S. T.; Shiba, Y.; Sarpong, R.; Keasling, J. D. Production of the Antimalarial Drug Precursor Artemisinic Acid in Engineered Yeast. *Nature* **2006**, *440*, 940–943.
- (38) Trenchard, I. J.; Smolke, C. D. Engineering Strategies for the Fermentative Production of Plant Alkaloids in Yeast. *Metab. Eng.* **2015**, *30*, 96–104.
- (39) Li, M.; Schneider, K.; Kristensen, M.; Borodina, I.; Nielsen, J. Engineering Yeast for High-Level Production of Stilbenoid Antioxidants. Sci. Rep. 2016, 6, 36827.
- (40) Hampton, R. Y. ER-Associated Degradation in Protein Quality Control and Cellular Regulation. *Curr. Opin. Cell Biol.* **2002**, *14*, 476–482.
- (41) Sandig, G.; Kärgel, E.; Menzel, R.; Vogel, F.; Zimmer, T.; Schunck, W.-H. Regulation of Endoplasmic Reticulum Biogenesis in Response to Cytochrome P450 Overproduction*,†. *Drug Metab. Rev.* 1999, 31, 393–410.
- (42) Bond, C. M.; Tang, Y. Engineering Saccharomyces Cerevisiae for Production of Simvastatin. *Metab. Eng.* **2019**, *51*, 1–8.
- (43) Li, Y.; Smolke, C. D. Engineering Biosynthesis of the Anticancer Alkaloid Noscapine in Yeast. *Nat. Commun.* **2016**, *7*, 12137.
- (44) Bat-Erdene, U.; Billingsley, J. M.; Turner, W. C.; Lichman, B. R.; Ippoliti, F. M.; Garg, N. K.; O'Connor, S. E.; Tang, Y. Cell-Free Total Biosynthesis of Plant Terpene Natural Products Using an Orthogonal Cofactor Regeneration System. *ACS Catal.* **2021**, *11*, 9898–9903.
- (45) McCoy, E.; O'Connor, S. E. Directed Biosynthesis of Alkaloid Analogs in the Medicinal Plant Catharanthus Roseus. *J. Am. Chem. Soc.* **2006**, *128*, 14276–14277.
- (46) Bernhardt, P.; McCoy, E.; O'Connor, S. E. Rapid Identification of Enzyme Variants for Reengineered Alkaloid Biosynthesis in Periwinkle. *Chem. Biol.* **2007**, *14*, 888–897.
- (47) Runguphan, W.; Qu, X.; O'Connor, S. E. Integrating Carbon-Halogen Bond Formation into Medicinal Plant Metabolism. *Nature* **2010**, *468*, 461–464.
- (48) McCoy, E.; Galan, M. C.; O'Connor, S. E. Substrate Specificity of Strictosidine Synthase. *Bioorg. Med. Chem. Lett.* **2006**, *16*, 2475–2478.
- (49) Gietz, R. D.; Schiestl, R. H. High-Efficiency Yeast Transformation Using the LiAc/SS Carrier DNA/PEG Method. *Nat. Protoc.* **2007**, *2*, 31–34.
- (50) Horwitz, A. A.; Walter, J. M.; Schubert, M. G.; Kung, S. H.; Hawkins, K.; Platt, D. M.; Hernday, A. D.; Mahatdejkul-Meadows, T.;

Szeto, W.; Chandran, S. S.; Newman, J. D. Efficient Multiplexed Integration of Synergistic Alleles and Metabolic Pathways in Yeasts via CRISPR-Cas. *Cell Syst.* **2015**, *1*, 88–96.

□ Recommended by ACS

Constructing Microbial Hosts for the Production of Benzoheterocyclic Derivatives

Xu-Liang Bu, Min-Juan Xu, et al.

JULY 29, 2020

ACS SYNTHETIC BIOLOGY

READ 🗹

Extrachromosomal Genetic Engineering of the Marine Diatom Phaeodactylum tricornutum Enables the Heterologous Production of Monoterpenoids

Michele Fabris, Peter Ralph, et al.

FEBRUARY 07, 2020

ACS SYNTHETIC BIOLOGY

READ 🗹

A Golden-Gate Based Cloning Toolkit to Build Violacein Pathway Libraries in Yarrowia lipolytica

Yingjia Tong, Peng Xu, et al.

JANUARY 05, 2021

ACS SYNTHETIC BIOLOGY

READ 🗹

Adaptive Optimization Boosted the Production of Moenomycin A in the Microbial Chassis Streptomyces albus J1074

Xing Li, Qianjin Kang, et al.

SEPTEMBER 01, 2021

ACS SYNTHETIC BIOLOGY

READ 🗹

Get More Suggestions >